



Kaolin-nano scale zero-valent iron composite(K-nZVI): synthesis, characterization and application for heavy metal removal

L. Sivarama Krishna^{a,b,c,d,*}, K. Soontarapa^{a,b}, A. Yuzir^c, V. Ashok Kumar^a, W.Y. Wan Zuhairi^d

^aDepartment of Chemical Technology, Faculty of Sciences, Chulalongkorn University, Pathumwan, Bangkok, 10330, Thailand, email: svurams@gmail.com (L.S. Krishna), Khantong.S@chula.ac.th (K. Soontarapa), rvashok2008@gmail.com (V.A. Kumar)

^bCenter of Excellence on Petrochemical and Materials Technology

^cDepartment of Environmental Engineering and Green Technology (EGT), Malaysia-Japan International Institute of Technology (MJIT) Universiti Teknologi Malaysia, Jalan Sultan Yahya Petra, 54100 Kuala Lumpur, email: muhdaliyuzir@utm.my (A. Yuzir)

^dGeology program, School of Environmental Science and Natural Resources, Faculty of Science and Technology (FST), University Kebangsaan Malaysia, Bangi-43600, Selangor, Malaysia, email: wanzuhairi@yahoo.com (W.Y.W. Zuhairi)

Received 8 January 2017; Accepted 5 December 2017

ABSTRACT

The present study explored the synthesis of Kaolin-nano scale zero-valent iron composite (K-nZVI) by using chemical reduction method. Sorption characteristics of the K-nZVI for the removal of Cu(II) ions was studied in batch conditions. The physical and chemical structure of the K-nZVI composite was characterized by Fourier transform infrared spectroscopy (FTIR), Scanning electron microscopy with energy dispersive X-ray spectroscopy (SEM-XRF), X-ray diffraction (XRD), Transmission electron microscopy (TEM) and Brunauer-Emmett-Teller studies (BET). The effect of pH, the initial metal ion concentration, and contact time on adsorption of Cu(II) onto K-nZVI was investigated. The K-nZVI exhibited good sorption performances over the initial pH range from 2.5 to 6.5. The kinetics data was studied by applying two sorption kinetic models (Pseudo-first and Pseudo-second-order) equations. The pseudo-second-order model was relatively suitable for describing the adsorption process. The equilibrium adsorption data is well fitted to Langmuir adsorption models. The maximum adsorption capacities of K-nZVI sorbent as obtained from Langmuir adsorption isotherm is found to be 178–200 mg g⁻¹ for Cu(II). Sorption isotherm models (Langmuir and Freundlich) were applied to the experimental data. The adsorption kinetics was well represented by the pseudo second order rate equation, and the adsorption isotherms were better fitted by the Langmuir equation. The thermodynamic studies showed that the adsorption reaction of Cu(II) is endothermic processes. The K-nZVI having number of features including easy preparation, environmentally friendly nature, low-cost and good sorption performance enable K-nZVI application in industrial purpose specifically in the field of industrial water treatment.

Keywords: K-nZVI composite; Heavy metal removal; Wastewater treatment; Adsorption

1. Introduction

Day-by-day increases pollution in environment, due to rapid industrialization in present modern world. Past few years researchers have focused on the development of efficient multifunctional materials with low-cost for various industrial applications. However, natural clays were abundantly available all over the world, they have different features, such as

low-cost, resource abundant, eco-friendly and porous nature towards, its application in various field. Hence extensive research has been focused on utilization of natural clay materials, chemically modified clays and clay-nano composites are widely used for wastewater treatment technology. However the utilization clay-nano composites for wastewater treatment is an interesting subject in recent years, a number of recent studies highlighted on the application of clay-nano composites, which used for various toxic pollutants removal (Dyes and metals) [1–6].

*Corresponding author.

The presence of copper in wastewater is toxic for aquatic flora and fauna even at very low concentrations (above 1.3 mg/l). According to the Safe Drinking Water Act (SDWA), the permitted limit of copper in drinking water is about 1.3 mg/l. Copper is an essential trace element that is more vital to the health of living things. However, it is acknowledge that excessive intake of copper results in many health risks and side effects. Those are including stomach and mucosal irritation, liver and kidney failure, intestine problems, neurotoxicity, mucosal irritation, wide spread capillary damage, depression, weakness, lethargy and anorexia, as well as damage to the gastrointestinal tract and lung cancer. The removal of copper from wastewater is a major problem due to the difficulty in treating of wastewaters by using conventional treatment methods [7–10].

Copper is mainly discharged into water bodies from various industrial activities such as metal cleaning and plating baths, brass manufacturing, pulp, paper and paper-board mills, electroplating industry, metal plating, metallurgical, smelting, mining activities, battery manufacture, tanneries, wood pulp production and copper-based agricultural chemicals etc. Hence, the removal of copper from wastewater is emergency need and, to protection of the aquatic environment [11,12].

Several methods have been developed for heavy metals removal from aqueous solutions, including chemical precipitation, ion exchange, chemical reduction, ultrafiltration, membrane separation, electrolysis, and adsorption [13]. Among them, adsorption is considered as superior method, because of its high efficiency and economic feasibility. Recently, adsorption technique has become an effective alternative method for the removal of various toxic pollutants [14–18].

However, in recent years, materials modified with nanoscale zero-valent iron with size of <100 nm has attracted great attention of many researchers owing to their potential applications. The efficiency of using nZVI for the removal of organic and inorganic pollutant from wastewater has been studied [19,20]. Recently it is used for the treatment of toxic contaminants in ground water and wastewater. However, due to its lack of stability and durability, mechanical strength, easy aggregation, and difficulty in separation from the treated solution, nZVI has limit uses [21–23]. To overcome these limitations, the researchers have attempt to use nZVI synthesized with solid porous materials such as activated carbon, resin, and clay minerals like bentonite, kaolinite and zeolite to remove different pollutants from aqueous solution.

So far, however, few studies have focused on this particular field, the present investigations demonstrate the synthesis of K-nZVI nano composite. The adsorption behaviors of Cu(II) onto K-nZVI nano composite was studied under different experimental conditions using batch method. In addition, different optimizing parameters such as doses, pH, initial concentration, contact time, temperature effect, thermodynamic parameters and desorption studies were extensively investigated. The adsorption equilibrium was evaluated by Langmuir and Freundlich adsorption isotherm models. Kinetic and thermodynamic parameters were also calculated. The prepared K-nZVI nano composite

was characterized by various analytical techniques and studied the physico-chemical properties. The K-nZVI nano composite exhibited as an efficient adsorption for Cu(II) from aqueous solution.

2. Experimental

2.1. Materials

Natural kaolin and the other following mentioned chemicals were provided by The Geochemistry Laboratory. All chemicals and solvents used in this study are of analytical grade quality. Iron (III) chloride hexahydrate ($\text{FeCl}_3 \cdot 6\text{H}_2\text{O}$, 99%, Sigma-Aldrich), copper sulphate (CuSO_4), lead (II) nitrate ($\text{Pb}(\text{NO}_3)_2$), sodium borohydride (NaBH_4 , 98% Sigma-Aldrich), absolute ethanol, HNO_3 , NaOH 99% and HCl were used in this study. These chemicals were analytical grade and applied without any further purification. Deionized and distilled water were used throughout the experiments. The Cu(II) stock solution was prepared by dissolving the prescribed amount of corresponding metal salts in double distilled water. Desired concentration of standard solutions was obtained by dilution of stock solution with double distilled water.

2.2. Preparation of the K-nZVI nano-composite

In this study, we prepared effective K-nZVI nano-composite was prepared using Fe(III) reduction method. In a first step, kaolin clay was dried in electric oven for 3 h at 55°C . The dried kaolin material was sieved using a molecular sieve and the <75 μm size of fraction was used in further reactions.

In second step, 4 grams of kaolin was transfer into 250 mL beaker. In another beaker 80 mL of ferric chloride solution was prepared by dissolving 4.83 g of ferric chloride with deionized water and absolute ethanol (1:1 liquid ratio). The obtained solutions were poured onto 4 grams kaolin powder. Then, the mixture was dispersed with an ultrasonic processor for 40 min to ensure a proper dispersion of iron particles onto the surface of kaolin. The mixture was subsequently stirred vigorously at room temperature for 40 min using magnetic shaker set at a speed of 180 rpm.

In third step, to obtain mixture, 3.549 g of freshly NaBH_4 dissolved in 60 mL of deionized water was dropped wisely into the mixture during the stirring and to continue stirring another 30 min. The reduction reaction is given in Eq. (1). After incubation, the black solids were separated from the solution using a vacuum filtration flask (Buchner funnel, Whatman qualitative filter paper, No.113, Size; 185 μm), washed three times with deionised water and ethanol respectively. The solid was then dried into the oven for 21 h at 55°C .



2.3. Techniques of characterization

The presence of functional group on the surface of materials was observed by Fourier transform infrared spectrometer (Model Perkin Elmer GX; spectrum BX). The IR spectra

of the materials were recorded from 4000 to 400 cm^{-1} wave number range. The crystalline structure of K-nZVI was checked by means of X-ray diffraction (Bruker, D8 Advance diffractometer, Germany) over a scanning interval (2 θ) from 5° to 9°. The surface morphology of the materials was examined with scanning electron microscopy/energy dispersive X-ray spectroscopy (ZEISS; service identification program (SIP); No. MNTS 0008). Dispersive X-Ray(EDX) system recorded at 5, 20 and 50 KX magnifications. The chemical compositions of the elements within the kaolin and K-nZVI were determined by EDX. FE-SEM + EDX were used at ETH = 3 KV for surface structure studies and EDX were operated under an acceleration voltage of 9 KeV. Regardless of FESEM analysis, the morphology of kaolin and K-nZVI and the sizes of Fe⁰ particles in the K-nZVI nano-composite were also characterized by transmission electron microscopy (TEM Philips). It was operated at 100 kV and magnification of 10,000; 13,000; 17,000; 22,000 and 35,000 times. The Brunauer Emmett and Teller (BET-N₂ adsorption-desorption isotherms) method was employed to measure the surface area, pore size and pore volumes of all samples (Model ASAP 2020 micro metrics). The concentration of metal ions (Cu(II)) in aqueous solution was determined by Atomic Adsorption Spectrometer (Perkin Elmer, 3300, Max, power 230 W; line voltage 50/60 Hz).

2.4. Batch adsorption procedure

Batch adsorption experiments were conducted in a rotatory and thermostatic shaker to determine the optimum operational parameters like; initial pH, contact time, initial metal concentration and temperature effect. The experiments were carried out using 25 mL of metal solution with constant adsorbent dose a constant temperature. For all adsorption tests, the initial pH values of the metal solution were adjusted using 0.1 M HCl or 0.1 M NaOH solutions. The removal percentage (% removal) and the equilibrium adsorption capacity (q_e) of K-nZVI were calculated by using the following equations:

$$\text{Removal percentage} = [(C_0 - C_e)/C_0] * 100 \quad (2)$$

where C_0 and C_e are liquid phase and equilibrium concentration of heavy metals in solution (mg L^{-1}).

The amount of adsorption at time t , q_t (mg g^{-1}), was calculated by

$$q_t = [(C_0 - C_t) V]/W \quad (3)$$

where C_0 and C_t (mg L^{-1}) are liquid phase concentrations of heavy metals at initial and at any time t , respectively, V is the volume of the solution (L) and W is the mass of dry adsorbent used (g).

2.5. Effect of adsorbent dose

In 50 ml polyethylene centrifuge tubes containing 50 mg/L of 25 ml of Cu(II) metal ion solutions 0.01–0.1 g of K-nZVI was introduced. The samples were agitated for 1 h at room temperature. The pH of metal ion solutions was used the suspensions at natural pH condition. The samples

were agitating on rotary shaker at 2000 rpm for 2 h, at room temperature. After agitation samples were centrifuged at 3000 rpm for 10 min and supernatant kept for Cu(II) analysis. The amounts of metal ion adsorbed by the adsorbents were calculated by difference.

2.6. Effect of pH

Twenty five milliliters of 50 mg/L of metal ion solutions was added to 0.05 g of K-nZVI was added in 50 ml polyethylene tubes. The pHs of the suspensions were adjusted within the pH range of 1.5–6.5 using either 0.1 M HCl and 0.1 NaOH M. These samples were agitated for 2 h. After agitation, the suspensions were centrifuged at 3000 rpm for 10 min and supernatant kept for Cu(II) analysis. The amount of metal ions adsorbed by the adsorbents was calculated.

2.7. Adsorption kinetic study

The pH of the metal ion solutions were adjusted to pH 3. Batch adsorption kinetic experiments were performed at room temperature on a rotary shaker at 200 rpm using 50 ml capped polyethylene tubes containing 25 ml of 10–40 mg/l of Cu(II) metal ion solutions and 0.05 g of K-nZVI adsorbent agitated at contact times 5, 10, 15, 20, 25, 30, 45 and 60 min. After agitation, the suspensions were centrifuged at 3000 rpm for 10 min and supernatant kept for Cu(II) analysis.

2.8. Adsorption equilibrium and thermo dynamic study

The pH of the Cu(II) metal ion solutions was adjusted to pH 3. Batch adsorption experiments were performed at different temperatures (25–55°C) on a rotary shaker at 200 rpm using 50 ml capped polyethylene tubes containing 25 ml of 50, 75, 100, 150 and 200 mg/l of metal ion solutions and 0.02 g of K-nZVI adsorbents for 1 h. After agitation, the suspensions were centrifuged at 3000 rpm for 10 min and supernatant kept for Cu(II) concentration analysis.

2.9. Adsorption isotherms

The sorption isotherm studies provide a relationship between the ion concentration in the solution and the amount of ion adsorbed on the solid phase at same temperature when the two phases reach the equilibrium. The sorption isotherms are mathematical models that were used to obtain the vital information such as sorption mechanism, surface properties and the affinity between the metal ions with the adsorbent. The two parameter isotherm models Langmuir and Freundlich were used by nonlinear regression methods to explain the sorption equilibrium data.

2.10. Langmuir isotherm model

$$(C_e/q_e) = (1/Q_{\max} K_L) + (C_e/Q_{\max}) \quad (4)$$

where Q_{\max} is the maximum biosorption capacity of K-nZVI (mg/g) and K_L is the Langmuir constant related to the sorption energy (L/mg).

2.11. Freundlich isotherm model

Freundlich isotherm model was also applied to describe the sorption of metal ions. Linearized in logarithmic form of Freundlich isotherm model equation is represented by:

$$\log q_e = \log K_F + (1/n) \log C_0 \quad (5)$$

where K_F is the Freundlich constant and '1/n' is the heterogeneity factor.

2.12. Kinetic models

The pseudo-first-order kinetic model, also known as the Lagergren kinetic equation as expressed in Eq. (6) and pseudo-second order model Eq. (7) have been widely used to predict sorption kinetics. The pseudo-first-order equation is generally applicable to the initial stage of the adsorption processes whereas the pseudo-second order equation predicts the behaviour over the whole range of adsorption.

$$\text{Log} (q_e - q_t) = \text{Log} q_e - (k_1/2.303)t \quad (6)$$

where q_e and q_t are the amounts of metals adsorbed at equilibrium and at time t (mg/g), respectively and k_1 is the pseudo first order rate constant (1/min). The pseudo-second-order kinetic model is given by equation:

$$t/q_t = (1/k_2 q_e^2) + (1/q_e)t \quad (7)$$

where, k_2 is the equilibrium rate constant of pseudo-second-order model (g/mol/min).

2.13. Thermodynamic parameters

The thermodynamic parameters such as Gibb's free energy (ΔG°), enthalpy change (ΔH°) and change in entropy (ΔS°) of Cu(II) is adsorbed by the K-nZVI was determined by following equations:

$$\Delta G^\circ = -RT \ln K_c \quad (8)$$

$$\text{where } K_c = C_s/C_e \quad (9)$$

$$\ln K_c = (\Delta S^\circ/R) - (\Delta H^\circ/RT) \quad (10)$$

where C_s is the equilibrium concentration of metal ions on adsorbent (mg/l), C_e is the equilibrium concentration of metal ions in solution (mg/l), K_c is the equilibrium constant, R is the ideal gas constant (8.314 J/mol/K) and T is the adsorption temperature in Kelvin.

3. Results and discussion

3.1. Characterization of the composite

The FE-SEM and TEM images of kaolin and K-nZVI composite are shown in Figs. 1a, 1b and 2a, 2b. The FE-SEM and TEM image of kaolin (Figs. 1a and 2a). shows that the surface morphology of kaolin is approximately smooth and

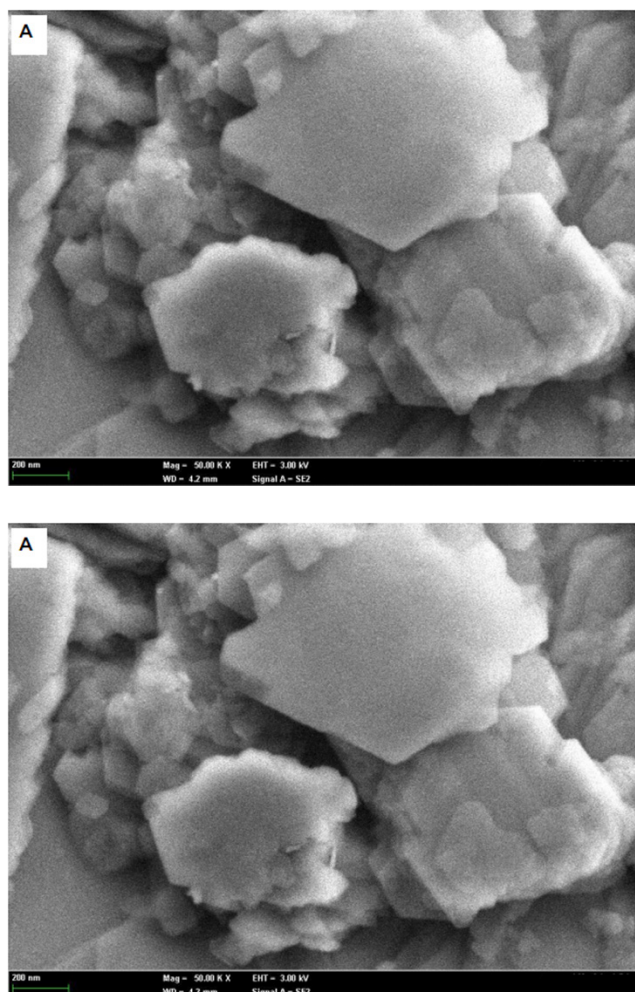


Fig. 1. SEM images of (A) kaolin and (B) K-nZVI.

homogenous. Figs. 1b and 2b demonstrate the dispersed well with little aggregation in the kaolin and the nZVI was present in chain-like structures. This led to confirm the successful attachment of nZVI with kaolin. The image 1.d has shown the crystal's size of Fe^0 particles range from 15.34–44.92 nm with an average size of 29.95 nm. The small black points in the picture shown (Fig. 2b) indicate the distribution of Fe^0 nanoparticles over the surface of kaolin in the composite like chain structure.

The surface areas and pores volume of kaolin and K-nZVI values are shown in Table 1. As expected, the BET surface area and pore volume are increased from kaolin to K-nZVI. Increasing surface area from 3.824 to 9.275 m^2/g from kaolin to K-nZVI was confirmed the formation of new porous structures and suggests that the Fe-nano particles were successfully synthesized on the kaolin and occupied the pores in kaolin.

The EDX test result shown in Figs. 3a and 3b, further confirmed the presence of elemental compound in the kaolin and as well as Fe nanoparticles without any impurity peaks. Different element spectra and their weight percentages are exist. Al and C were mostly derived from the inorganic constituents of kaolinite. The Fe-nano particles are obviously existed on the K-nZVI composite (7.75%)

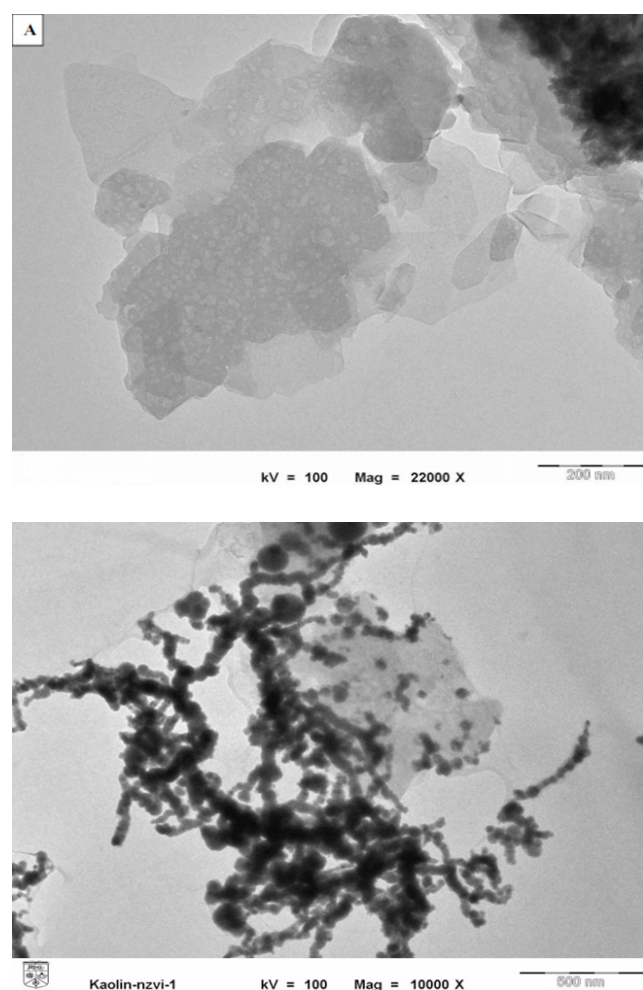


Fig. 2. TEM images of (A) kaolin and (B) K-nZVI.

Table 1
BET analysis of kaolin and K-nZVI

Samples	Surface area m ² /g	T plot micropore volume cm ³ /g	Adsorption average pore width	Adsorption cumulative volume of pores cm ³ /g
Kaolin	3.824	1.8 × 10 ⁻⁵	171.75	0.022
K-nZVI	9.276	0.026	111.32	0.0325

shown in Fig. 3b. The increased of the Fe content in K-nZVI composite compared to bare kaolin (0.69%) to confirm the synthesizing of K-nZVI nano composite. The iron and weak oxygen signals in the EDX spectrum was recorded, these signals are to confirm the formation of Fe-nano particles on the kaolin dominated as zero-valent iron, Fe⁰ and to form K-nZVI nano composite (Fig. 3b) [23].

The XRD patterns of kaolin and K-nZVI are shown in Figs. 4a and 4b, respectively. The XRD patterns in Fig. 3a show that the kaolin composed of minerals such as kaolinite as the major clay mineral and quartz as a non-clay mineral. Many other minerals were also observed such as mullite,

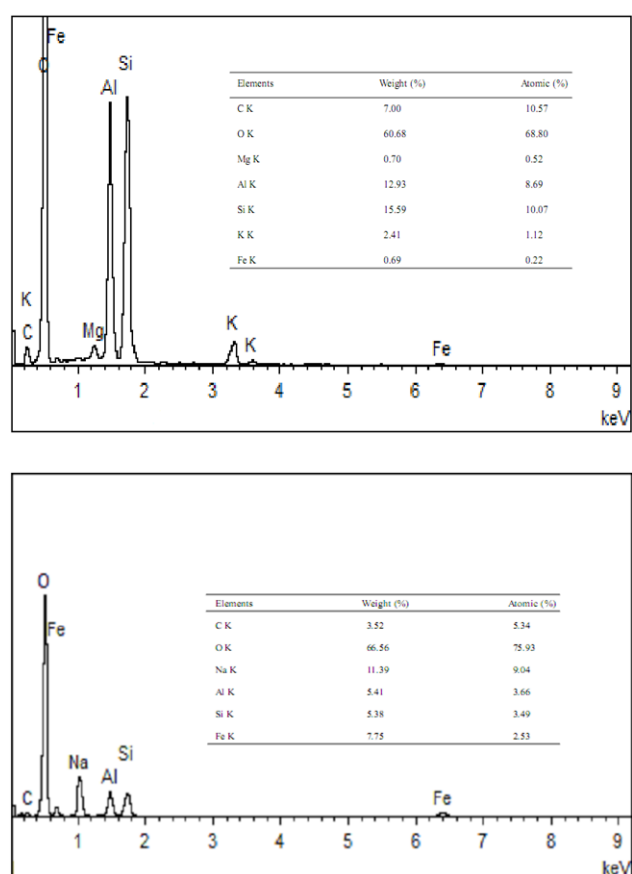


Fig. 3. EDX images of (A) Kaolin and (B) K-nZVI.

nacrite, dickite, pyrophyllite, dobassite, schwertmannite, staurolite and chloritoid, respectively. Comparing to kaolin, K-nZVI has some new diffraction peaks, Fig. 4b shows that at $2\theta = 44.66^\circ$ and 44.77° [24] and $2\theta = 64.97^\circ$, 65.03° and 65.24° [25] were corresponded to the formation of iron in its zero-valent iron (Fe⁰ states 110 and 200; JCPD no. 87-0721). This indicated that Fe⁰ nanoparticles were supported on the kaolin surface. The present of iron in other form of maghemite Fe₂O₃ at $2\theta = 17.63$, 37.76 , 39.28 and 44.9 . It's indicating that n-ZVI loaded onto kaolin was covered by a layer of iron oxides. At the same time, Fe formed many other compounds with silicon and alumina such as aluminium iron fersilicite, almandine, akaganeite, cronstedtite and iron silicon. At different points which was seen in the same peaks with quartz and kaolinite in the software that detected the reflections. These reflections indicate the presence of Fe from ferric chloride on the surface of kaolin. The Fe³⁺ adsorbed by the kaolin was probably reduced to Fe⁰ and immobilized on the surface. The XRD analysis indicates the formation of the composite and immobilization of Fe⁰ and its well dispersion onto the composite in chain form.

The FTIR spectrum for kaolin and K-nZVI composite were scanned in the range of 4000–400 cm⁻¹ as shown in Figs. 4a and 4b respectively. Figs. 5a and 5b show the bands at 3400–3696 cm⁻¹ in kaolin and K-nZVI corresponding to OH stretching of inner surface of hydroxyl groups. This is present as OH molecules in octahedral

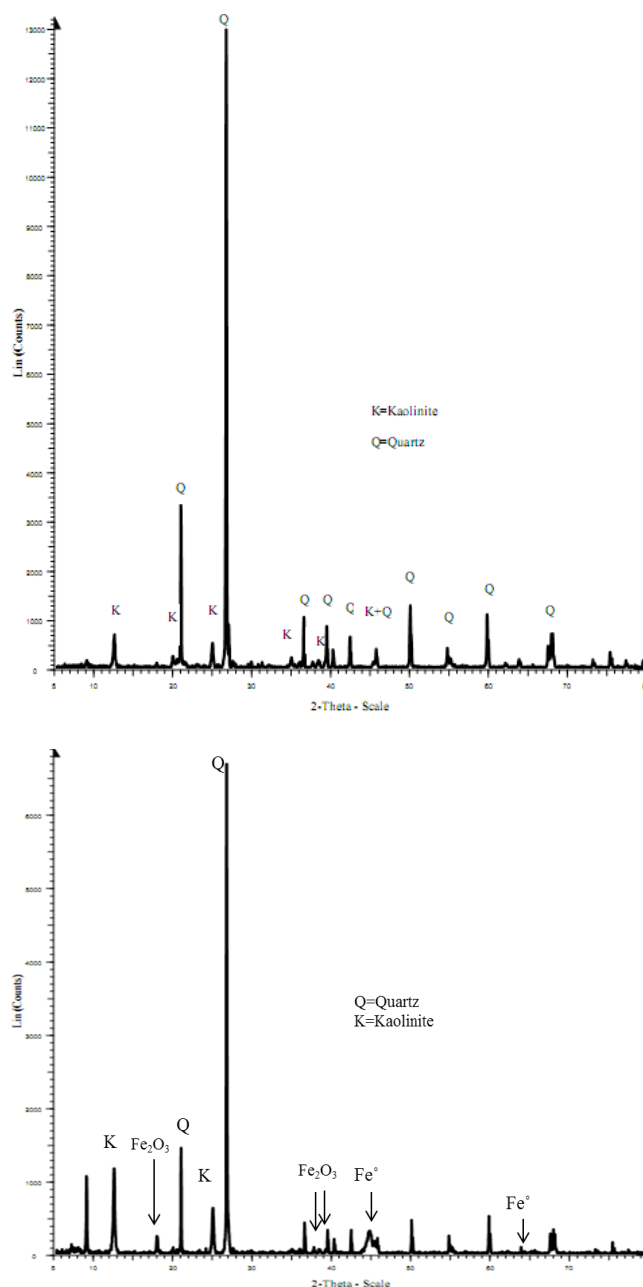


Fig. 4. XRD images of (A) Kaolin and (B) K-nZVI.

layer of kaolin. Bands at 3619.49 cm^{-1} in kaolin represent as OH stretching of inner hydroxyl groups group. Bands at $1018.46\text{--}1107.63\text{ cm}^{-1}$ can be attributed to Si-O stretch. Bands at $1032\text{--}1008$ can be attributed to in-plane Si-O-stretching, band at 915 cm^{-1} is O-H deformation of inner hydroxyl groups and 930 cm^{-1} Al-OH and finally bands at $788\text{--}693.48\text{ cm}^{-1}$ can be attributed to Si-O translation in kaolin. The K-nZVI FTIR spectrums shown clearly, the disappearance of many peaks which was exist in the raw kaolin, indicating the loss of water molecules in the composite. Band at 2304 cm^{-1} belongs to stretching of O-H groups and band at 1633.88 cm^{-1} can be attributed to H-O-H bonding. The peaks at $912\text{--}107\text{ cm}^{-1}$ in K-nZVI

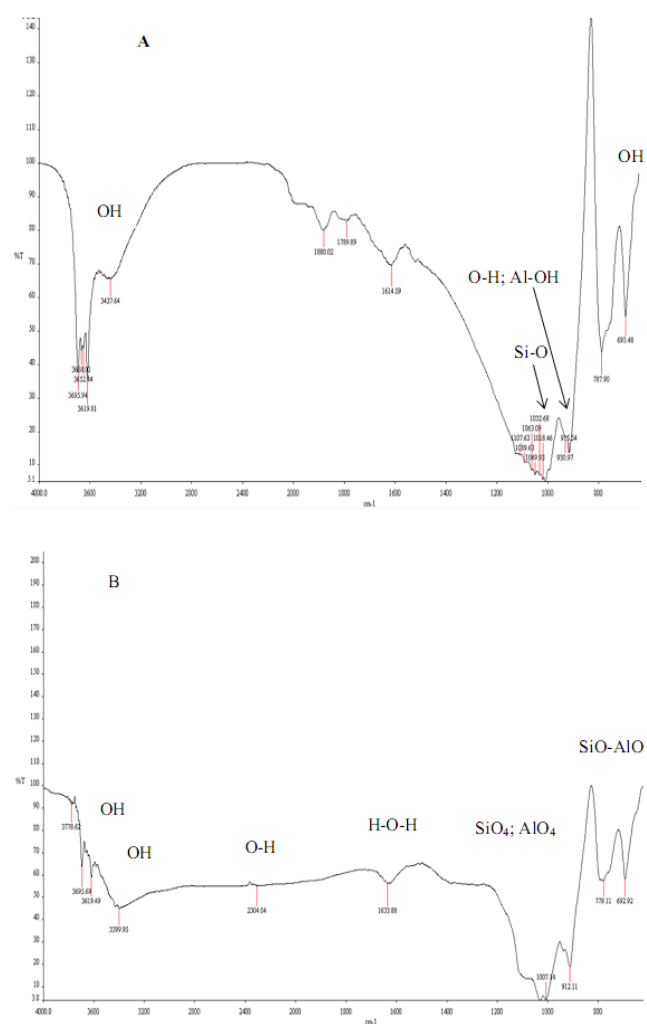


Fig. 5. FTIR analyses of (A) Kaolin and (B) K-nZVI.

and those at $915\text{--}930\text{ cm}^{-1}$ in kaolin indicating stretching of SiO_4 and AlO_4 in the kaolin. Many more bands disappeared in the K-nZVI between $915\text{--}1107\text{ cm}^{-1}$ imply to breaking of H bands due to the presence of Fe on the SiO_4 and AlO_4 surfaces of kaolin and finally bands at $693\text{--}779\text{ cm}^{-1}$ in K-nZVI and $693\text{--}788\text{ cm}^{-1}$ in kaolin indicating the Si-O and Al-O bonds [1,26,27]. A strong band shows at 779 cm^{-1} in K-nZVI attributable in part to iron oxides on the surface of kaolin. Its indicating less oxidation of K-nZVI formed [1]. This evidence also support to the SEM, TEM, EXD, XRD and BET.

3.2. Adsorption of Cu(II) on K-nZVI

3.2.1. Effect of K-nZVI dose

The effect of adsorbent (K-nZVI) on the removal of Cu(II) is shown in Fig. 6. The adsorption of metal efficiency is highly dependent on the quantity of the adsorbent. Several researchers reported that the increase in the percentage removal with increase in the adsorbent dosage is due to the greater availability of the exchange-

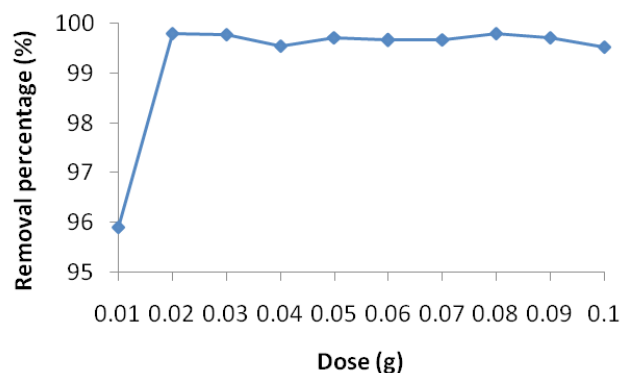


Fig. 6. Effect of K-nZVI dose.

able sites or more adsorption sites or more surface area at higher concentration of the adsorbent. The present study reveals, the adsorbent dosage of 0.02 g is optimum dose found to be uptake of the K-nZVI was 62.38 (99.8%) mg/g for Cu(II). After that the adsorption is constant due to the decrease in equilibrium adsorption capacity per unit mass of adsorbent with increasing the dosage may be due to the higher K-nZVI dose providing more active adsorption sites. Another possible reason is the decreased total surface area of the adsorbent and an increase in the diffusion path length caused by the aggregation of adsorbent particles [27].

3.2.2. Effect of initial pH

In adsorption process solution pH is one of the vital parameter that influences the surface charge and dissociation of functional groups on the adsorbent. In addition pH also affects the degree of ionization and speciation of the metal ions. Therefore it is essential to evaluate the optimum pH for the adsorption process of Cu(II) onto K-nZVI. Hence, 0.05 g of the K-nZVI composite was mixed with 25 mL of solution containing 50 mg/l Cu(II), at different pHs ranges from 1.5 to 6.5 at room temperature with agitation of 200 rpm for 2 h. The pH of the solutions was adjusted with 0.1 M NaOH and HCl before adding the K-nZVI composite. After agitation, the suspensions were centrifuged at 3000 rpm for 10 min, subsequently filtered and then, the supernatant acidified and kept in refrigerator prior to analysing. Fig. 7 indicates that the adsorption capacity of composite for Cu(II) is reached the adsorption maximum value of 24.68 mg/g (98.6%) at pH 2.5. It was observed that the pH beyond optimum level showed static saturated adsorption. Further slightly increase in amount of metals removal is observed. Owing to following reasons, more Fe(OOH) coating on K-nZVI surfaces or metal hydroxide precipitation can be deposited on K-nZVI surfaces. Copper metal ions are Cu^{2+} is the dominating chemical form up to pH of 7. To increase the metals solution pH, Cu^{2+} is to forms the metal hydroxides such as $\text{Cu}(\text{OH})^+$, $\text{Cu}_2(\text{OH})_2^{2+}$, $\text{Cu}_3(\text{OH})_4^{2+}$, $\text{Cu}(\text{OH})_3^+$ and $\text{Cu}(\text{OH})_2$. These hydroxides are electro statically attracted towards the composite of metal oxide [28]. These reasons had influence and decrease reactivity of Fe^0 . Thus adsorption experiments were optimized by adjusting the initial pH to 2.5 and were followed by reduction metal ions by

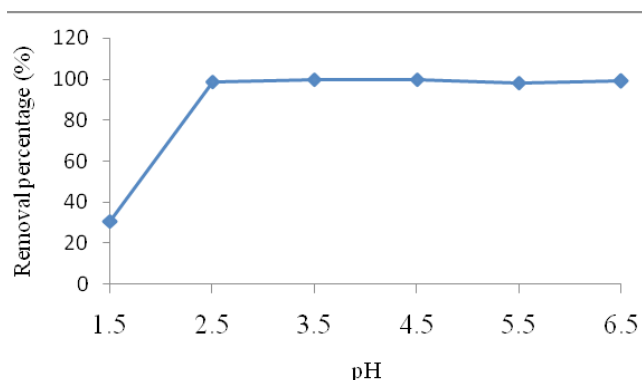


Fig. 7. Effect of varying pH on Cu(II) adsorption.

Fe^0 . Furthermore, the acidity of the solution can dissolution of the Fe(OOH) layer on nZVI surfaces and it is helpful to adsorb metal ions using K-nZVI [1].

3.3. Adsorption kinetics

3.3.1. Effect of contact time and initial metal concentration

In this experiment, the effect of agitation time on the adsorption of metal ions by the K-nZVI was explored. The samples were taken from the shaker at different time periods varying from 5, 10, 15, 20, 25, 30, 45 to 60 min for initial concentrations of Cu(II) 10–40 mg/l. The adsorption of Cu(II) ions as a function of shaking time at room temperature are presented in Figs 8. The time required for attaining equilibrium for Cu(II) ions was about 5 min. Maximum adsorption was attained as 99.9% for Cu(II) ion. From Fig. 8, an increase in the initial metal concentration leads to an increase in the amount of metal ion adsorbed onto K-nZVI. However, this may occur due to an increase in the driving force of the concentration gradient with the increase in the initial metal concentration. The results suggested that a rapid increase in Cu(II) adsorption occurred for the first 5 min then it get saturated and the curve almost remains constant. For the first 5 min agitation time, 99.9% of Cu(II) removal was obtained. Meanwhile, prolonged agitation was not resulted in higher removal efficiency. The removal percentage of Cu(II) increased from 99% (12.38 mg/g) to 99.6% (49.79) with increase in the initial concentration of Cu(II) ions from 10 to 40 mg/l.

This might be due to the interaction between metal ions present in the solution with binding site.

At lower metal ions concentration, the percentage uptake was higher due to the large surface area of adsorbent being available for adsorption. While the high concentration of metal ions, the percentage removal decreased since the available sites for adsorption became less due to saturation of adsorption sites. The higher initial concentrations might be closely associated with large values of the ratio between the initial concentration of metal ions and the limited number of available binding sites, resulting in lower adsorption percentage.

However, different from the percentage uptake, with the increasing initial metal ions concentration from 10 mg/l to 40 mg/l, the amount of metal ions adsorbed at

equilibrium increased. This occurred due to increase in driving force of the concentration gradient to overcome all mass transfer resistance of metal ions between aqueous and solid phases and accelerate the probable collision between metal ions and sorbents, thus resulting in higher uptake of metal ions. It can be concluded that 0.02 g K-nZVI is able to sufficiently remove Cu(II) from aqueous solution within concentrations of 10–40 mg/l. This result is important for considering the treatment of copper contain wastewaters and the other similar applications. The data obtained from the experiment was further used to evaluate the kinetic parameters of the adsorption process.

Pseudo-first-order equation, pseudo-second-order equation and intra-particle diffusion equation were used as kinetic models to analyze the adsorption behaviors of Cu(II) on K-nZVI. The pseudo-first-order kinetic model not fits. The pseudo-second-order kinetic model reflects the adsorbed amount at equilibrium and the adsorbed amount on the surface of the adsorbent. The intra-particle diffusion model involved in the adsorption process because it can identify the intra-particle diffusion mechanism and analyze the control steps in the adsorption.

The pseudo-second-order kinetic model for the removal of Cu(II) on K-nZVI values are summarized in Table 2. The correlation coefficient (R^2) of the pseudo-second-order equation was higher than that of pseudo-first-order equation. In addition, the values of the calculated q_e with different initial Cu(II) concentrations (10–40 mg/l), the q_e values 11.904, 24.390, 36.900, and 49.504 mg/g respectively to concentration of copper.

3.4. Thermodynamic studies

Thermodynamic parameter for the adsorption of Cu(II) is shown in Tables 3. The variation of metal ion removal efficiency with respect to different temperatures (25°C, 35°C, 45°C to 55°C) explained by the thermodynamic parameters such as Gibb's free energy (ΔG°), enthalpy change (ΔH°) and change in entropy (ΔS°) of Cu(II) adsorbed by the K-nZVI (Table 3). These parameters are can be determined using equations. Where R is (8.314 J/mol K) is the gas constant and T (K) the absolute temperature. The values of ΔS° and ΔH° are calculated from the slopes and intercepts of plots of $\ln K_c$ versus $1/T$. The slope of the plot equal to $\Delta H^\circ/R$ and its intercept is equal to $\Delta S^\circ/R$. The ΔG° , ΔH° and ΔS° are shown in Table 3. The enthalpy of the adsorption ΔH° mean is a measure of the energy barrier that must be overcome by reacting molecules. The values for ΔH° were found to be in the range of 21.12–24.74 KJ/mol and positive values. This suggests that the adsorption reactions of Cu(II) onto K-nZVI is endothermic in nature meaning that increasing temperature will favour the adsorption of Cu(II) metal onto the K-nZVI. The value of ΔS° mean is an indication of whether or not the adsorption reaction is by associative or dissociative mechanism. The ΔS° value is very small that means the entropic change occurring during adsorption process is negligible. The positive value of ΔS° indicates the increased entropy at the solid or solution interface [29] during the adsorption and fixation of Cu(II) on the active sites of K-nZVI and correspond to an increase in the degree of freedom of the adsorbed species.

Table 2

Calculated value of Cu(II) kinetic mechanism using pseudo second-order

C_0 mg/l	q_e	K_2	R^2
10	11.904	-0.019	0.999
20	24.390	-0.004	0.999
30	36.900	-0.002	0.999
40	49.504	-0.0009	0.999

Table 3

Thermodynamic parameters of Cu(II) on K-nZVI conditions

Temperature	ΔG° (Kj/mol)	ΔH° (Kj/mol)	ΔS° (Kj/mol)
25	21.109	21.124	4.9×10^{-5}
35	22.337	22.352	
45	22.390	22.406	
55	24.723	24.739	

3.5. Adsorption isotherms

Adsorption isotherms are generally used as reference points to evaluate the characteristic performance of an adsorbent. Subsequently, there are many isotherm models have been used for the equilibrium modeling of adsorption systems. The results obtained from the empirical studies were applied to Langmuir and Freundlich isotherms. The dependence of C_e versus C_e/q_e and $\log C_e$ vs. $\log q_e$ were plotted (Figures not shown) using empirical results.

The Langmuir and Freundlich constant values of different initial concentrations (50, 75, 100, 150 and 200 mg L^{-1}) at different temperatures (25°C, 35°C, 45°C and 55°C) for Cu(II) shown in Table 4. The values of the parameters and correlation coefficient (R^2) of Cu(II) are summarized in Table 4. It is noted that the Langmuir isotherm model exhibits better fit to the adsorption of Cu(II) over the Freundlich isotherm model. The value of Q_{max} determined from the Langmuir model increases with increase in temperature. The results indicate the confirming that the process of adsorption is endothermic. These results supporting to the thermodynamic results.

Freundlich isotherm constants n and K_f for Cu(II) are calculated at different temperatures from the slope and intercept of the plots, $\log C_e$ versus $\log q_e$ and the values presented in Table 4. The R^2 values of Freundlich isotherm from Table 4 indicate that this model has not been able to adequately describe the relationship between the amounts of Cu(II) adsorbed by the K-nZVI and its equilibrium concentration in the solution. The adsorption capacity, K_f was found to increase with an increase in temperature and this suggests that adsorption process is endothermic in nature. The values of n between 1 and 10 represent a favourable sorption. In the present study the values of n also follows the same trend. Higher the value of $1/n$, higher will be the affinity between the adsorbate and adsorbent and thus reveal heterogeneity of the adsorbent sites. However, this model also fits better for equilibrium data since it presents higher R^2 value.

Table 4
Adsorption isotherms values for the removal of Cu(II) on K-nZVI

Langmuir constants				Freundlich constants		
Temp.	Q_{max} mg/g	K_L (L/mg)	R^2	K_F	n	R^2
25	178.57	0.00019	0.971	3.84	4.49	0.962
35	181.83	0.00016	0.989	3.55	3.46	0.948
45	188.68	0.00020	0.983	3.61	3.37	0.869
55	200.00	0.00110	0.966	4.00	3.86	0.936

4. Conclusions

This study provides the detailed investigation on the synthesis of K-nZVI Nano-composite and characterization. The composite was synthesized using low-cost abundant Kaolin clay waste material and K-nZVI using for Cu(II) removal from aqueous environment successfully. The K-nZVI can be successfully employed as adsorbent for Cu(II) removal from aqueous solution. The result of BET has shown the increasing of surface area from kaolin to K-nZVI. The results of XRD, SEM and TEM images confirm the synthesis of the composite. The pH, initial metal ion concentration, K-nZVI dosage, contact time and temperature were found to have a significant effect on the adsorption efficiency of Cu(II). The adsorption capacity is maximum at pH 5.0 and decreases significantly either side of pH 2.5. Among the two kinetic equations applied, the kinetic data tended to fit well to the pseudo-second-order rate model. The maximum adsorption capacity is 200 mg g⁻¹ at higher temperature. The thermodynamic constants ΔG° , ΔH° and ΔS° of the adsorption process have shown that adsorption of Cu(II) ions on K-nZVI are endothermic and spontaneous. The present work demonstrates that the K-nZVI is potential adsorbent for application in the removal of Cu(II) ions. The synthesis methods, economic nature, ease of separation, and good adsorption performance of K-nZVI for potential application in industrial application form metal ions removal from aqueous.

Acknowledgments

The authors are grateful to the Graduate School School and The Thailand Research Fund (IRG578001), Chulalongkorn University for providing financial support, Postdoctoral Fellowship under Rachadapisaek Sompote Fund.

References

- [1] S.A. Kim, S.K. Kannan, K.J. Lee, Y.J. Park, P.J. Shea, W.H. Lee, H.M. Kim, B.T. Oh, Removal of Pb(II) from aqueous solution by a zeolite-nanoscale zero-valent iron composite, *Chem. Eng. J.*, 217 (2013) 54–60.
- [2] Y. Zhang, Y. Li, J. Li, L. Hu, X. Zheng, Enhanced removal of nitrate by a novel composite: nanoscale zero valent iron supported on pillared clay, *Chem. Eng. J.*, 171 (2011) 526–531.
- [3] S. Lee, K. Lee, S. Rhee, J. Park, Development of a new zero-valent iron zeolite material to reduce nitrate without ammonium release, *J. Environ. Eng.*, 133 (2007) 6–12.
- [4] W. Wang, M. Zhou, Q. Mao, J. Yue, X. Wang, Novel NaY zeolite-supported nanoscale zero-valent iron as an efficient heterogeneous Fenton catalyst, *Catal. Commun.*, 11 (2010) 937–941.
- [5] S. Wang, Y. Peng, Natural zeolites as effective adsorbents in water and wastewater treatment, *Chem. Eng. J.*, 156 (2010) 11–24.
- [6] X. Zhang, S. Lin, X.Q. Lu, Z.L. Chen, Removal of Pb(II) from water using synthesized kaolin supported nanoscale zero-valent iron, *Chem. Eng. J.*, 163 (2010) 243–248.
- [7] B. Acemioglu, M.H. Alma, Equilibrium studies on the adsorption of Cu(II) from aqueous solution onto cellulose, *J. Colloid Interface Sci.*, 243 (2001) 81–84.
- [8] M. Mohapatra, L. Mohapatra, P. Singh, S. Anand, B.K. Mishra, A comparative study on Pb(II), Cd(II), Cu(II), Co(II) adsorption from single and binary aqueous solutions on additive assisted nano-structured goethite, *Int. J. Eng. Sci. Technol.*, 2 (2010) 89–103.
- [9] S. Rengaraj, J.W. Yeon, Y. Kim, Y. Jung, Y.K. Ha, W.H. Kim, Adsorption characteristics of Cu(II) onto ion exchange resins 252H and 1500H: Kinetics, isotherms and error analysis, *J. Hazard. Mater.*, 143 (2007) 469–477.
- [10] US EPA, Cost and benefits of reducing lead in gasoline, Draft final report, Office of policy analysis, US EPA 230-03-84-005, Washington, DC, 1984.
- [11] T. Theophanides, J. Anastassopoulou, Copper and carcinogenesis, critical reviews, *Oncology/Haematology*, 42(1) (2002) 57–64.
- [12] Y. Li, B. Xia, Q. Zhao, F. Liu, P. Zhang, Q. Du, D. Wang, D. Li, Z. Wang, Y.i. Xia, Removal of copper ions from aqueous solution by calcium alginate immobilized kaolin, *J. Environ. Sci.*, 23(3) (2011) 407–410.
- [13] P. Cañizares, Á. Pérez, R. Camarillo, Recovery of heavy metals by means of ultrafiltration with water-soluble polymers: calculation of design parameters, *Desalination*, 144 (2002) 279–285.
- [14] L. Sivarama Krishna, M. Jagadeesh, M.C. Sivasankar Reddy, W.Y. Wan Zuhairi, M.R. Taha, A. Varada Reddy, Evaluation of biomass, Indian Jujuba seed (IJS) for removal of Congo red (CR), *Am. J. Environ. Sci.*, 10 (2014) 374–382.
- [15] L. Sivarama Krishna, A. Sreenath Reddy, A. Muralikrishna, W.Y. Wan Zuhairi, H. Osman, A. Varada Reddy, Utilization of the agricultural waste (Cicerarientinum Linn fruit shell biomass) as biosorbent for decolorization of Congo red, *Desal. Water Treat.*, 56(8) 2181–2192.
- [16] L. Sivarama Krishna, A. Sreenath Reddy, W.Y. Wan Zuhairi, M.R. Taha, A. Varada Reddy, Indian Jujuba seed powder as an eco-friendly and a low-cost biosorbent for removal of Acid Blue 25 from aqueous solution, *The Sci. World J.*, 11 (2014) 2014.
- [17] N. Das, Remediation of radionuclide pollutants through bio-sorption-an overview, *CLEAN – Soil, Air, Water*, 40 (2012) 16–23.
- [18] M.C.S. Reddy, L. Sivarama Krishna, A. Varada Reddy, The use of an agricultural waste material, jujuba seeds for the removal of anionic dye (Congo Red) from aqueous medium, *J. Hazard. Mater.*, 203–204 (2012)118–127.
- [19] X.Q. Li, D.W. Elliott, W.X. Zhang, Zero-valent iron nanoparticles for abatement of environmental pollutants: materials and engineering aspects, *Crit. Rev. Solid State Mat. Sci.*, 31 (2006) 111–122.
- [20] Y.P. Sun, X.Q. Li, J. Cao, W.X. Zhang, H.P. Wang, Characterization of zero-valent iron nanoparticles, *Adv. Colloid Interface Sci.*, 120 (2006) 47–56.
- [21] L. Cumbal, J. Greenleaf, D. Leun, A.K. Sen Gupta, Polymer supported inorganic nanoparticles: characterization and environmental applications, *React. Funct. Polym.*, 54 (2003) 167–180.
- [22] J.T. Nurmi, P.G. Tratnyek, V. Sarathy, D.R. Baer, J.E. Amonette, K. Pecher, C. Wang, J.C. Linehan, D.W. Matson, R.L. Penn, M.D. Driessen, Characterization and properties of metallic ion nanoparticles: spectroscopy, electrochemistry, and kinetics, *Environ. Sci. Technol.*, 39 (2005) 1221–1230.
- [23] L. Zhang, A. Manthiram, Ambient temperature synthesis of fine metal particles in montmorillonite clay and their magnetic properties, *Nano struct. Mater.*, 7 (1996) 437–451.

- [24] N. Arancibia-Miranda, S.E. Baltazar, A. García, D. Muñoz-Lira, P. Sepúlveda, M.A. Rubio, D.A. Facultad, Nanoscale zero valent supported by Zeolite and Montmorillonite: Template effect of the removal of lead ion from an aqueous solution, *J. Hazard. Mater.*, 301 (2016) 371–380.
- [25] S. Lee, K. Lee, S. Rhee, J. Park, Development of a new zero valent iron zeolite material to reduce nitrate without ammonium release, *J. Environ. Eng.*, 133 (2007) 6–12.
- [26] L. Vaculikova, E. Plevova, S. Vallova, I. Koutnik, Characterization and differentiation of kaolinites from selected Czech deposits using infrared spectroscopy and differential thermal analysis, *Acta Geodyn. Geomater.*, 8 (2011) 59–67.
- [27] E.I. Unuabonah, K.O. Adebawal, B.I. Olu-Owolabi, L.Z. Yang, L.X. Kong, Adsorption of Pb (II) and Cd (II) from aqueous solutions onto sodium tetraborate-modified Kaolinite clay: Equilibrium and thermodynamic studies, *Hydrometallurgy*, 93 (2008) 1–9.
- [28] X.Q. Li, W.X. Zhang, Sequestration of metal cations with zerovalent iron nanoparticles - a study with high resolution X-Ray photoelectron spectroscopy (Hr-Xps), *J. Phys. Chem. C*, 111 (2007) 6939–6946.
- [29] L.-n. Shi, X. Zhang, Z.-l. Chen, Removal of chromium (VI) from wastewater using bentonite-supported nanoscale zero-valent iron, *Water Res.*, 45 (2011) 886–887.
- [30] Y. Chang, Y.-y. He, T. Liu, Y.-h. Guo, F. Zha, Aluminum pillared palygorskite-supported nanoscale zero-valent iron for removal of Cu(II), Ni(II) from aqueous solution, *Arab. J. Sci. Eng.*, 39(2014) 6727–6736.